

The semi-Lagrangian technique in atmospheric modelling: current status and future challenges

Michail Diamantakis

*ECMWF, Shinfield Park, Reading
RG2 9AX, United Kingdom
michail.diamantakis@ecmwf.int*

ABSTRACT

The semi-Lagrangian method is an established numerical technique for integrating the transport equations in atmospheric models. Coupled with semi-implicit time-stepping offers unconditional stability for all forcing terms in equation sets of such models. This distinct advantage has led to the development of very efficient numerical weather prediction systems such as the ECMWF Integrated Forecasting System (IFS).

The highly accurate spectral transform, semi-Lagrangian IFS has been operating for over two decades and has been continuously updated and improving. In this article, the main algorithms underpinning semi-Lagrangian models are reviewed and work that continuously evolves towards improving these is summarized. Emphasis is placed on current research topics such as noise problems in the stratosphere, the extratropical tropopause cold bias and mass conservation. Finally, the question whether a semi-Lagrangian formulation can be a viable choice at future super-computing architectures is briefly discussed.

1 Introduction

The semi-Lagrangian (SL) method is a widely used numerical technique for solving the transport equations in global weather prediction models. It is an unconditionally stable scheme which exhibits very good phase speeds and little numerical dispersion. The practical result of these theoretical properties is that it allows stable integrations with long timesteps, at CFL numbers much larger than unity, without distorting the important Rossby waves. When a SL scheme is coupled with a semi-implicit (SI) time discretization, long timesteps can be used in realistic atmospheric flow conditions where a multitude of fast and slow processes coexist. Furthermore, the virtues of the Lagrangian and Eulerian approach are combined in a single scheme: although a Lagrangian approach is used for advection, the transported fields are remapped at every timestep to the model grid. The undesirable side-effects of large grid deformation of the purely Lagrangian approach is therefore limited and physical processes can be accurately computed.

The SLSI approach is currently the most popular option for operational global Numerical Weather Prediction (NWP) models while it is often used in limited area modelling. Some examples of well known global SLSI models in alphabetical order are: ARPEGE (Meteo France), GEM (Environment Canada), GFS (NCEP), GSM (JMA), IFS (ECMWF), MetUM (UKMO). SLSI numerics have been used in the ECMWF forecast model (IFS) since 1991. As discussed by [Simmons \(1991\)](#), the change from Eulerian to semi-Lagrangian numerics improved the efficiency of IFS by a factor of six enabling thus a significant resolution upgrade at that time. Since 1991, further successful upgrades followed and currently the (high resolution) forecast model is run at 16 km resolution in grid-point space.

For a detailed description of the benefits of semi-Lagrangian modelling the reader can refer to the review paper by [Staniforth and Côté \(1991\)](#). Here, we introduce the basic algorithms used in semi-Lagrangian

computations with an emphasis in IFS formulation. This allows to demonstrate strengths and weaknesses of the SLSI approach and to discuss work towards improving further the quality of weather forecasts within the framework of IFS.

2 Semi-Lagrangian solution of the advection problem

To present in a simple way the basic ideas underpinning the semi-Lagrangian method we consider the continuity equation for a tracer field χ which predicts how its density ρ_χ changes as it is transported by a wind field \mathbf{V} :

$$\frac{D\rho_\chi}{Dt} = -\rho_\chi \nabla \cdot \mathbf{V}, \quad \frac{D}{Dt} = \frac{\partial}{\partial t} + \mathbf{V} \cdot \nabla, \quad \mathbf{V} = (u, v, \dot{\eta}). \quad (1)$$

In (1) $\dot{\eta}$ denotes the vertical component of the wind, i.e. the derivative of the [Simmons and Burridge \(1981\)](#) hybrid vertical coordinate η , a monotonic function of pressure which is terrain following near the surface and flat near the top of the atmosphere.

It is common practice in SL models to use specific ratios $\phi_\chi = \rho_\chi / \rho$ rather than ρ_χ . Here, ρ is the air density which satisfies the continuity equation:

$$\frac{D\rho}{Dt} = -\rho \nabla \cdot \mathbf{V}. \quad (2)$$

Using specific ratios, with the aid of (2), we can transform equation (1) in the simple pure advective (without source terms) form:

$$\frac{D\phi_\chi}{Dt} = 0. \quad (3)$$

Integrating (3) along the trajectory a fluid parcel follows in the time interval $[t, t + \Delta t]$,

$$\int_t^{t+\Delta t} D\phi_\chi = 0,$$

results to:

$$\phi_{\chi,a}^{t+\Delta t} = \phi_{\chi,d}^t.$$

Subscript letters a, d denote the so-called arrival and departure points. The former is the location of a parcel at time $t + \Delta t$ and coincides with a grid-point. One timestep before, at time t , this parcel is at d . Therefore, it is assumed that at each timestep, parcels depart from points d to arrive at grid-points. The location of d is somewhere in the space between grid-points and has to be found. Therefore, to compute the field at the new timestep $t + \Delta t$ it suffices to compute a departure point for each grid-point and find (interpolate) the values of the transported field at these departure points.

In the equations that follow, for notational convenience, the arrival point subscript a will be omitted. The basic steps in a semi-Lagrangian algorithm which solves the transport equation (3) are:

1. For each grid-point solve the following trajectory equation for the departure point (d.p.) \mathbf{r}_d :

$$\frac{D\mathbf{r}}{Dt} = \mathbf{V}(\mathbf{r}, t) \Rightarrow \underbrace{\mathbf{r}}_{\text{arrival g.p.}} - \underbrace{\mathbf{r}_d}_{\text{unknown d.p.}} = \int_t^{t+\Delta t} \mathbf{V}(\mathbf{r}, t) dt \quad (4)$$

2. Remap (interpolate) ϕ to \mathbf{r}_d to obtain

$$\phi^{t+\Delta t} = \phi_d^t$$

2.1 Finding departure points

Solving the trajectory equation (4) requires the numerical approximation of a velocity integral. The mid-point rule is a commonly used approach:

$$\mathbf{r} - \mathbf{r}_d = \Delta t \mathbf{V} \left(\frac{\mathbf{r} + \mathbf{r}_d}{2}, t + \frac{\Delta t}{2} \right). \quad (5)$$

The time-dependent discrete trajectory equation (5) is solved for \mathbf{r}_d which is the d.p. of the grid-point \mathbf{r} . The velocity field value at the trajectory mid-point and at time $t + \Delta t/2$ must be found first. The usual technique is to use time-extrapolation and then interpolate the extrapolated velocity field at the estimated mid-point. The second order extrapolation formula is often used:

$$\mathbf{V}^{t+\Delta t/2} = \mathbf{V}^t + \frac{\Delta t}{2} \frac{\partial \mathbf{V}^t}{\partial t} + O(\Delta t^2) = \mathbf{V}^t + \frac{\Delta t}{2} \frac{\mathbf{V}^t - \mathbf{V}^{t-\Delta t}}{\Delta t} + O(\Delta t^2) \approx 1.5\mathbf{V}^t - 0.5\mathbf{V}^{t-\Delta t}$$

Summarizing, after the extrapolated field $\mathbf{V}^{t+\Delta t/2}$ has been computed, the following fixed-point iteration algorithm can be used to compute the departure point:

1. Initialise: $\mathbf{r}_d^{(1)} = \mathbf{r} - \Delta t \mathbf{V}^t$
2. For $\ell = 2, \dots, L$:
 - (a) Interpolate $\mathbf{V}^{t+\Delta t/2}$ to mid-point $\mathbf{r}_m \equiv 0.5[\mathbf{r} + \mathbf{r}_d^{(\ell-1)}]$
 - (b) Update: $\mathbf{r}_d^{(\ell)} = \mathbf{r} - \Delta t \mathbf{V}^{t+\Delta t/2}(\mathbf{r}_m)$

Linear interpolation has been found to provide sufficiently accurate results for the interpolation of the wind field in step 2(a) and it is the preferred option in most semi-Lagrangian models (Staniforth and Côté, 1991). Furthermore, in IFS, step 2 is replaced by

$$\mathbf{r}_d^{(\ell)} = \mathbf{r} - \frac{\Delta t}{2} \left[\mathbf{V}^{t+\Delta t/2}(\mathbf{r}_d^{(\ell-1)}) + \mathbf{V}^{t+\Delta t/2}(\mathbf{r}) \right]$$

i.e. the mid-point wind is replaced by an average along the trajectory as according to Temperton et al. (2001) the latter was found to reduce noise problems.

Pudikiewicz et al. (1985) give a sufficient condition for convergence of the above iterative procedure. Quoting Staniforth and Côté (1991) this Lipschitz condition is that “the timestep Δt should be smaller than the reciprocal of the absolute maximum value of the wind-shear at each direction”. The geometric interpretation of this condition, given by Smolarkiewicz and Pudykiewicz (1992), is that trajectories do not intersect each-other. In practice this is satisfied for atmospheric flows and two iterations are enough to obtain satisfactory (second order) accuracy, i.e. there is no further practical advantage by keep iterating.

2.2 Interpolation

Essentially, through the SL discretization the advection problem is turned to an interpolation one. Although linear interpolation is sufficiently accurate for the wind field when solving the trajectory equation, a high order scheme must be used for interpolating a transported field ϕ to the departure points. As noted by Staniforth and Côté (1991) cubic Lagrange has been found to be a good compromise between computational cost and accuracy.

In IFS, instead of using a three-dimensional formula which is expensive, interpolation is applied at each dimension separately. For example, on the sphere, interpolation to a d.p. $(\lambda_d, \theta_d, \eta_d)$ is done as a sequence of three separate one-dimensional interpolations in λ_d (longitude), θ_d (latitude) and finally η_d . The aim of the first interpolation is to find the field values at the d.p. longitude. These interpolated values, all at the same longitude λ_d , are then interpolated to the d.p. latitude. Finally, the outcome of the previous interpolations which represents values at the same longitude and latitude (vertically aligned) is interpolated to η_d to obtain the interpolated field value at d . A three dimensional computational stencil of neighbouring points (to the d.p.) is used. For a full cubic interpolation 64 points are required while for the quasi-cubic interpolation used in IFS 32 are sufficient. Details can be found in the paper by [Ritchie et al. \(1995\)](#). A quasi-monotone limiter such as the one by [Bermejo and Staniforth \(1992\)](#) is often used to avoid generating new maxima or minima in the solution and avoid unphysical oscillations (shape preservation).

3 Two time-level semi-Lagrangian semi-implicit integration

Having introduced the basic ideas behind semi-Lagrangian numerics we will now extend these to equation sets which include forcing terms such as the primitive hydrostatic set of IFS.

Consider the following set of prognostic equations (momentum components, temperature, continuity, tracers):

$$\frac{D\mathbf{X}}{Dt} = \mathbf{F}(\mathbf{X}), \quad \mathbf{X} = (X_1, X_2, \dots, X_M) \quad (6)$$

where M denotes the number of equations in the set and \mathbf{F} is the forcing term. Integrating (6) along a trajectory,

$$\frac{\mathbf{X}^{t+\Delta t} - \mathbf{X}_d^t}{\Delta t} = \int_t^{t+\Delta t} \mathbf{F}(\mathbf{X}(t)) dt \quad (7)$$

and approximating the right-hand side integral using the second order trapezoidal scheme the following SLSI discretization is obtained:

$$\frac{\mathbf{X}^{t+\Delta t} - \mathbf{X}_d^t}{\Delta t} = \frac{1}{2} (\mathbf{F}_d^t + \mathbf{F}^{t+\Delta t}) \quad (8)$$

where the subscript d implies interpolation to the departure point. Equation (8) is an expensive and complex one to solve due to its large dimension, its implicitness and in general its non-linear form (right hand-side \mathbf{F} includes non-linear terms). For this reason the approach used is to extract fast terms from the right-hand side (e.g. the ones corresponding to gravity waves, or in the non-hydrostatic case the acoustic terms as well) and linearise them around a constant reference profile. The right-hand side of the forcing term is split to:

$$\mathbf{F} = \mathbf{N} + \mathbf{L}$$

where \mathbf{L} contains the linearised and fast linear terms which will be integrated implicitly and \mathbf{N} the remaining non-linear terms $\mathbf{N} = \mathbf{F} - \mathbf{L}$ which will be integrated explicitly. Following [Temperton et al. \(2001\)](#), the two-time-level second order discretization of (8) may be written:

$$\frac{\mathbf{X}^{t+\Delta t} - \mathbf{X}_d^t}{\Delta t} = \frac{1}{2} (\mathbf{L}_d^t + \mathbf{L}^{t+\Delta t}) + \frac{1}{2} (\mathbf{N}_d^{t+\Delta t/2} + \mathbf{N}^{t+\Delta t/2}). \quad (9)$$

The nonlinear terms at $t + \Delta t/2$ are computed by the same second order extrapolation formula used in the departure point calculation:

$$\mathbf{N}^{t+\Delta t/2} = 1.5\mathbf{N}^t - 0.5\mathbf{N}^{t-\Delta t}.$$

Once the right-hand side of (9) has been evaluated the semi-implicit system can be solved. To avoid solving simultaneously all implicit equations in set (9), a Helmholtz equation is derived from these. In

spectral transform IFS this is formulated as a constant matrix coefficient problem in terms of horizontal divergence (see [Ritchie et al., 1995](#)). Using properties of spherical harmonics the Helmholtz equation can be solved very efficiently in spectral space. Once divergence has been corrected by the Helmholtz solver then all prognostic variables can be updated through back-substitution.

3.1 Iterative Centred Implicit Scheme

The advantage of the approach described in section 2.1 is its low computational cost. However, the extrapolations used may occasionally result in loss of stability which is manifested as noise in the stratosphere. One way to overcome this problem while maintaining second order accuracy is to use an iterative centred implicit approach (ICI) such as the one described by the following steps:

1. Apply standard semi-implicit scheme (9) with time-extrapolation where required to obtain a predictor for \mathbf{X} :

$$\mathbf{X}^{(0)} \approx \mathbf{X}^{t+\Delta t}.$$

2. For $k = 1, 2, \dots, K$ apply again the semi-implicit scheme but now using time-interpolation in place of extrapolation:

Use $\mathbf{V}^{t+\Delta t/2} = 0.5 [\mathbf{V}^{(k-1)} + \mathbf{V}^t]$, $\mathbf{V}^{(k-1)} \approx \mathbf{V}^{t+\Delta t}$ in trajectory solver iterations

Use $\mathbf{N}^{t+\Delta t/2} = 0.5 [\mathbf{N}^{(k-1)} + \mathbf{N}^t]$, $\mathbf{N}^{(k-1)} \approx \mathbf{N}^{t+\Delta t}$ in:

$$\frac{\mathbf{X}^{(k)} - \mathbf{X}_d^t}{\Delta t} = \frac{1}{2} (\mathbf{L}_d^t + \mathbf{L}^{(k)}) + \frac{1}{2} (\mathbf{N}_d^{t+\Delta t/2} + \mathbf{N}^{t+\Delta t/2})$$

3. At final iteration: $\mathbf{X}^{t+\Delta t} = \mathbf{X}^{(k)}$.

In practice, one extra iteration ($k = 1$) suffices to eliminate noise and obtain a stable solution. However, despite its benefits, the ICI scheme is avoided in operational IFS runs as it doubles the computational cost of the dynamics. Instead, the technique described in the following section is what is used operationally.

3.2 SETTLS: Stable Extrapolation Two-Time-Level Scheme

SETTLS by [Hortal \(2002\)](#) is a more stable alternative to the standard extrapolation technique analysed in previous sections which is also second order accurate. It is derived by a Taylor series expansion:

$$\Psi^{t+\Delta t} \approx \Psi_d^t + \Delta t \left(\frac{d\Psi}{dt} \right)_d + \frac{\Delta t^2}{2} \left(\frac{d^2\Psi}{dt^2} \right)_{AV}$$

where AV denotes an ‘‘average along the semi-Lagrangian trajectory’’ during the timestep from t to $t + \Delta t$.

If Ψ obeys $\frac{d\Psi}{dt} = R$, taking into account the approximation $\left(\frac{d^2\Psi}{dt^2} \right)_{AV} \approx \frac{R(t) - R_d(t - \Delta t)}{\Delta t}$ results to:

$$\Psi^{t+\Delta t} \approx \Psi_d^t + \frac{\Delta t}{2} (R^t + [2R^t - R^{t-\Delta t}]_d) \quad (10)$$

where the subscript d denotes interpolation to the departure point. Using Taylor series expansion we may verify that

$$R_m^{t+\Delta t/2} \approx \frac{1}{2} (R^t + [2R^t - R^{t-\Delta t}]_d)$$

is a second order accurate approximation at the trajectory mid-point m and at time $t + \Delta t/2$. Following [Hortal \(2002\)](#), formula (10) can be used for extrapolating the wind fields when solving the trajectory equation as well as for extrapolating the non-linear terms:

- to find departure points iterate:

$$\mathbf{r}_d^{(\ell)} = \begin{cases} \mathbf{r} - \Delta t \mathbf{V}^t, & \ell = 1 \\ \mathbf{r} - 0.5 \Delta t (\mathbf{V}^t + [2\mathbf{V}^t - \mathbf{V}^{t-\Delta t}]_d^{(\ell-1)}), & \ell > 1 \end{cases} \quad (11)$$

interpolating the square bracketed terms at latest available estimate of the departure point

- replace the non-linear terms in (9) by:

$$\mathbf{N}_m^{t+\Delta t/2} = 0.5 (\mathbf{N}^t + [2\mathbf{N}^t - \mathbf{N}^{t-\Delta t}]_d). \quad (12)$$

Operational implementation of SETTLS in IFS (April 1998) eliminated the noise problem in all areas except for the upper part of the stratosphere where it persisted in occasions in which the stratospheric night polar jet is shifted away from the poles. An example can be seen in Fig. 1 where the horizontal divergence field from a forecast at $t+24$ hrs, starting at $t = 15/01/2012$ 12 UTC, is plotted at heights of 5 hPa and 1 hPa. According to [Hortal \(2004\)](#) this noise can be attributed to a non-linear feedback between the extrapolatory mechanism for computing the vertical component of the departure point and the solution of the evolution equations. Although the associated instability is too weak to cause a model failure during a 10 day forecast and it is limited in the upper part of the stratosphere it does seem to seriously affect the data assimilation scheme: satellite data rejections occur due to a mismatch between the (noisy) background forecast fields and the observations. It is therefore important to eliminate this noise which was achieved introducing some smoothing of the vertical component of the velocity (see [Hortal, 2004](#)).

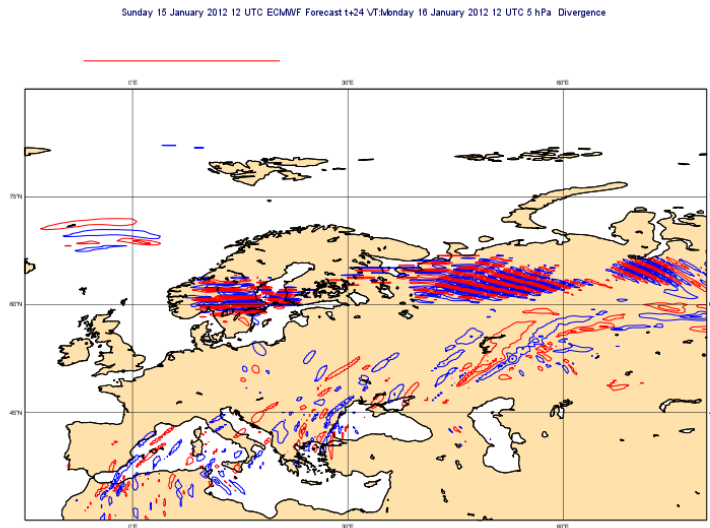


Figure 1: 5hPa horizontal divergence field at $t+24$ hrs from an IFS forecast starting at $t = 15/01/2012$ 12 UTC and using SETTLS.

3.3 Limiting SETTLS when computing trajectories

Vertical velocity smoothing improves the stability of the IFS SLSI scheme but it was found to cause a degradation of stratospheric skill scores. For this reason a filter for SETTLS scheme has been recently

developed to be applied at upper model levels (e.g. those at heights above 60 hPa) when computing the vertical component of the departure point. This scheme replaces (11) in the vertical only for $\ell > 1$ by:

$$\eta_{d^{[\ell]}} = \begin{cases} \eta - 0.5\Delta t \left(\dot{\eta}^t + [2\dot{\eta}^t - \dot{\eta}^{t-\Delta t}]_{d^{[\ell-1]}} \right), & |\dot{\eta}^t - \dot{\eta}^{t-\Delta t}| \leq 0.5\beta (|\dot{\eta}^t| + |\dot{\eta}^{t-\Delta t}|) \\ \eta - 0.5\Delta t \left(\dot{\eta}^t + \dot{\eta}_{d^{[\ell-1]}}^t \right), & |\dot{\eta}^t - \dot{\eta}^{t-\Delta t}| > 0.5\beta (|\dot{\eta}^t| + |\dot{\eta}^{t-\Delta t}|) \end{cases} \quad (13)$$

where, $0 < \beta < 2$. It is a composite between SETTLS and an alternative scheme which resembles the trapezoidal method:

$$\eta_d = \eta - 0.5\Delta t \left(\dot{\eta}^{t+\Delta t} - \dot{\eta}_d^t \right).$$

The difference is that $\dot{\eta}^{t+\Delta t}$ above is approximated by the simple first-order, one-term extrapolation $\dot{\eta}^{t+\Delta t} \approx \dot{\eta}^t$. Asymptotically, the principal difference between the two branches of (13) is

$$\frac{(\Delta t)^2}{2} \left(\frac{\partial \dot{\eta}}{\partial t} \right)_d^t$$

which is a small term when the vertical velocity is slowly changing in time.

The condition used in (13) is a simple criterion to decide which points have potential to develop instability. This heuristic rule essentially compares the magnitude of the $\dot{\eta}$ jump during two consecutive timesteps with a two-timestep average of the $\dot{\eta}$ magnitude. Big jumps are likely to be an indication of instability and when this occurs the alternative to SETTLS is activated. Second order, two-term extrapolations may have higher accuracy asymptotically than first order, one-term extrapolation schemes but are prone to instabilities.

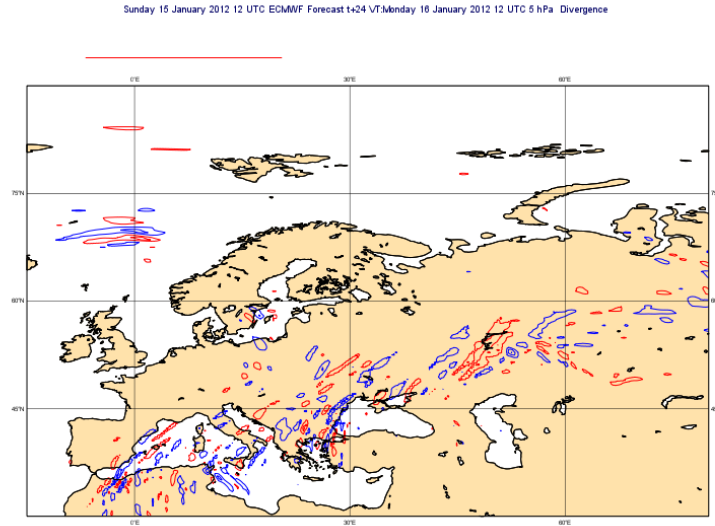


Figure 2: 5hPa horizontal divergence field at $t + 24$ hrs for a forecast starting at $t = 15/01/2012$ 12 UTC and using SETTLS filter.

The parameter β in (13) controls how strict is the test: for $\beta \geq 2$ SETTLS will be applied on all grid-points while for $\beta \leq 0$ the alternative scheme will be applied everywhere. Tests for different β values have been done suggesting that even a value as large as 1.99 is sufficient to stop the problem occurring. Values smaller than but near 2 penalize points that jump from negative to positive values within a timestep as well as those that maintain the same sign but exhibit big jumps. In this case only about 5% – 10% of the points per level were filtered i.e. SETTLS was switched off on these points. So, in

practice we maintain second order of accuracy in the trajectory calculation except for the points which are most likely to develop an instability.

The forecast corresponding to Fig. 1 has been repeated applying the new filter at upper model levels where the pressure falls below 60hPa. The results are plotted in Fig. 2 and demonstrate that noise has been completely eliminated. Furthermore, analysis experiments (4D-VAR trials) strongly indicate that use of this filter has a big positive impact in the forecast skill in the upper stratosphere and increases significantly the number of observations being assimilated due to the fact that these are not rejected. This is the result of enhanced stability leading to smooth temperature forecasts which have values close to observations. The impact is shown in Fig. 3 where it is evident that the temperature difference between the background forecast and observations is smallest when the filter is used. The velocity smoothing scheme improves noticeably but does not eliminate the problem.

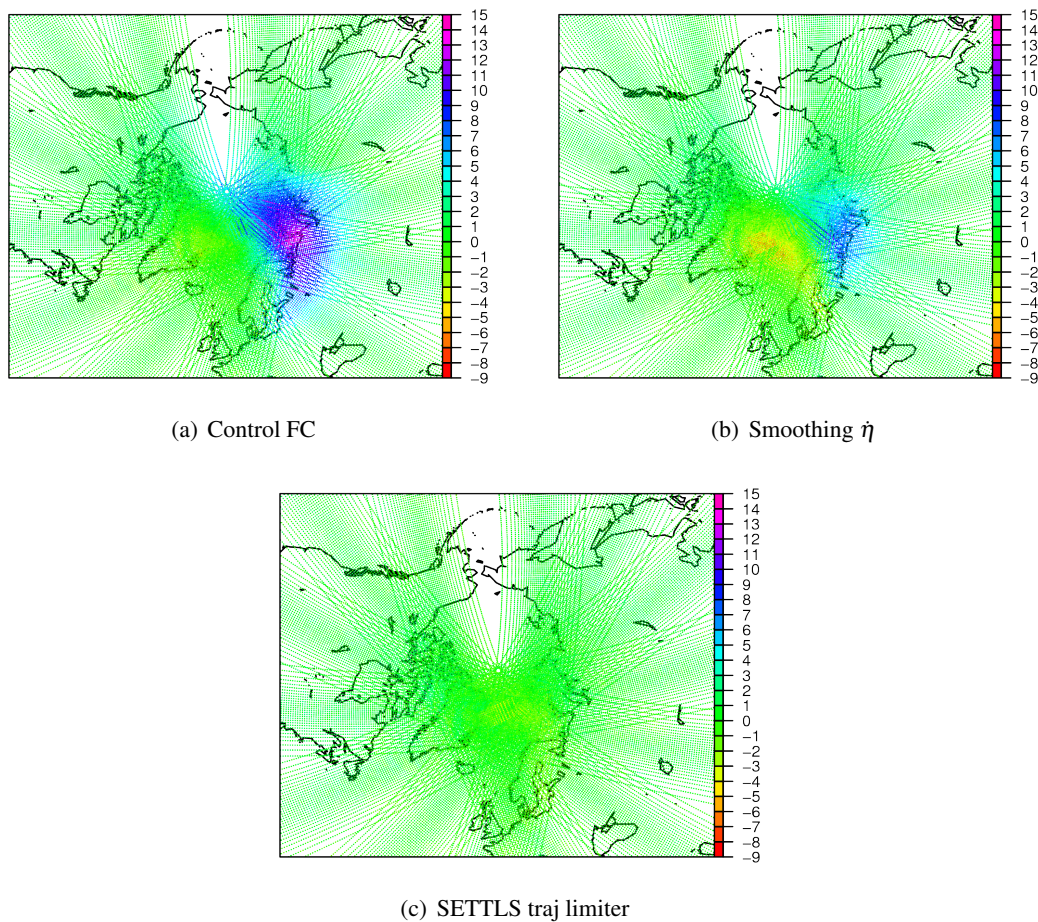


Figure 3: Temperature difference for METOP-A AMSU-A observations (channel 13) minus background forecast at $t = 12$ UTC 15/01/12.

4 The cold bias systematic error

The extra-tropical tropopause cold bias is a systematic error occurring in IFS as well as in other semi-Lagrangian models. As explained by [Stenke et al. \(2008\)](#) who investigated this problem using a semi-Lagrangian version of ECHAM4 GCM, this bias is due to water vapour overestimation in lower extratropical stratosphere which leads to radiative cooling. A significant contributing factor to this moist bias is the combination of enhanced horizontal numerical diffusion of semi-Lagrangian schemes and

the existing strong meridional gradient of water vapour between the tropical upper troposphere and the extratropical lowermost stratosphere. This diffusive behaviour can be attributed to the lack of adequate resolution to resolve accurately steep gradients and the diffusive properties of the interpolation schemes in general.

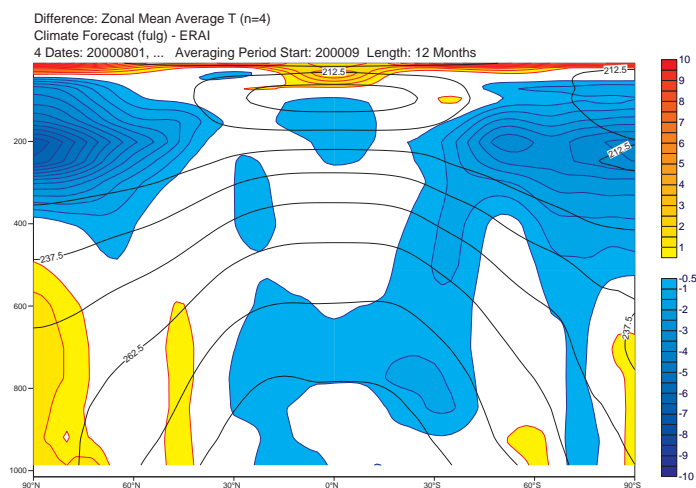


Figure 4: Forecast minus ERAI temperature field, zonally and time averaged, from four 12-month forecasts.

The cold bias can be clearly seen in Fig. 4 where the difference between the time averaged zonal mean of the temperature field for four twelve month forecasts and the corresponding ERAI (ERA interim) field is plotted. Tests recently done with IFS broadly agree with the findings of [Stenke et al. \(2008\)](#) and give further useful guidance on how to reduce the cold bias. Overall, they suggest that the modeled cold bias is a problem clearly sensitive to the numerical schemes applied in dynamics. Large sensitivity was found in the method used to interpolate horizontally the **specific humidity** field to the departure point and to the method used to interpolate the wind field during the departure point calculation.

The sensitivity with respect to the quasi-monotone limiter for specific humidity is striking. We remind that this is done to stop the interpolation scheme generating new local minimum and maximum values which are deemed artificial (although in some cases they may be actually true due to lack of sufficient resolution). Limiting the horizontal interpolation only and not the vertical part did not show any improvement. Removing both horizontal and vertical limiting had a big positive impact, i.e. it reduced the cooling. This shows in Fig. 5a. Furthermore, the following modifications to the quasi-monotone limiter were tested:

- (a) Using the standard [Bermejo and Staniforth \(1992\)](#) quasi-monotone limiter as opposed to the IFS default one (Fig. 5b). The difference is that the former is limiting the solution (interpolated values) after the three one-dimensional interpolations have been completed (in longitude, latitude, height) while the latter is limiting immediately after each one-dimensional interpolation.
- (b) Applying the same limiter as in (b) but also making a compensating correction for each grid-point field value which has been limited (Fig. 5c). Briefly this works as follows:
 1. Interpolate humidity field to the computed departure point
 2. Starting from top model level limit each grid-point at current level using Bermejo & Staniforth scheme and store the mass the limiter has removed from or added to the grid-point value.

3. The mass that has been removed/added by the limiter is added/removed at the grid-point directly below.
4. Move one level below and repeat the above process until reaching the level above surface.

This procedure has the additional benefit of improving mass conservation as no mass is lost or gained as a result of the action of the limiter.

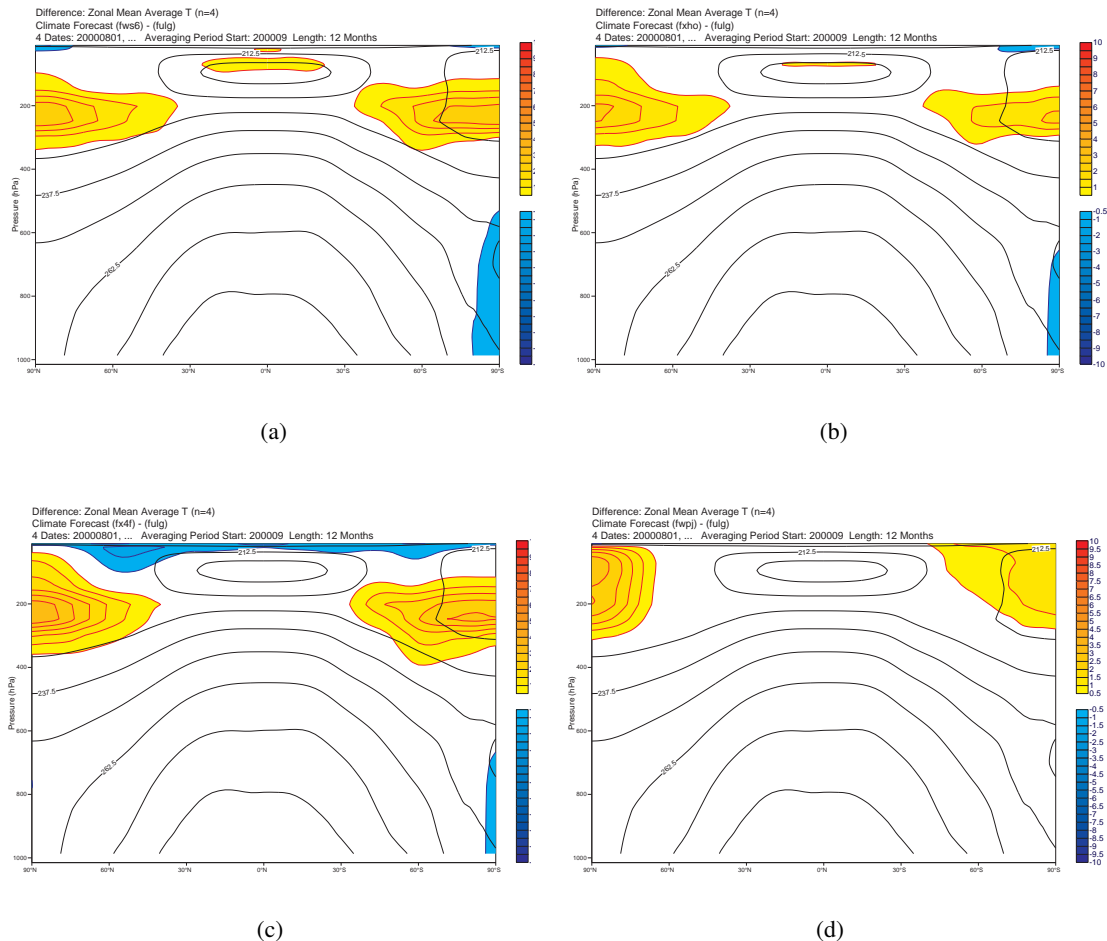


Figure 5: Difference of experiment from control of time averaged zonal mean temperature for runs with different dynamics options: (a) quasi-monotone limiter off and use of negative fixer (b) Bermejo & Staniforth quasi-monotone limiter (c) same as (b) but with compensating correction (d) cubic Hermite interpolation with derivative limiting in the vertical.

Using alternative schemes for interpolating in the vertical such as cubic Hermite interpolation with smoother, derivative limiting as suggested by Hyman (1983) also shows sensitivity and often a benefit (see Fig. 5d). However, the resulting warming spreads higher in the upper stratosphere in regions that there is already a warm bias.

Other “dynamics” parameters or schemes available in IFS have also been tested. Summarizing these tests, sensitivity was found in reducing the timestep, using ICI scheme, introducing off-centring in the semi-implicit scheme, switching off quasi-monotone limiter in the continuity equation (surface pressure advection). None of these tests demonstrated a benefit similar to the one found by changing the quasi-monotone limiter for specific humidity as discussed in the previous paragraph.

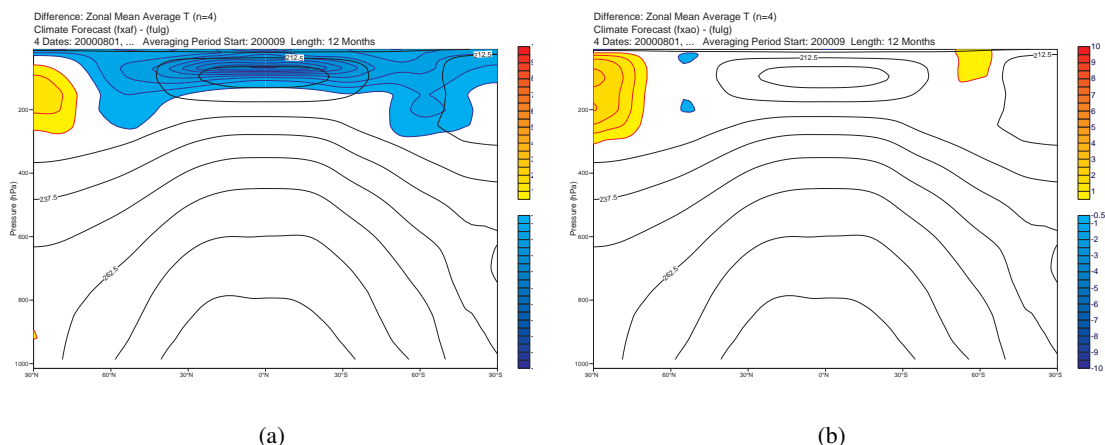


Figure 6: Difference of experiment from control (cf. Fig.5) when (a) smoothing vertical velocity is used and (b) when SETTLS filter is used.

The cold bias sensitivity with respect to options for solving the semi-Lagrangian trajectory equation has also been tested. In particular the impact of smoothing vertical velocities and of the SETTLS filter introduced in section 3. Results from these tests are shown in Fig. 6 and suggest that smoothing exaggerates the cooling while the SETTLS filter has a small benefit. In this test, the filter was applied from the top of the model atmosphere down to levels near the 100hPa pressure level.

5 Mass conservation in IFS

Conventional semi-Lagrangian transport schemes used in NWP cannot formally conserve mass. Lack of formal mass conservation is important for the long time integrations typical in climate simulations but is not crucial for short and medium range NWP forecasts. Due to the good accuracy of the SLSI method the resulting mass conservation error is usually small. For example, in a 10-day IFS forecast, at T1279 horizontal spectral resolution (approximately 16km in grid-point space) and 137 levels in the vertical, the total model air mass is increasing by less than 0.01% of its initial value. The formulation of the continuity equation in IFS, based on Ritchie and Tanguay (1996) scheme (see also ECMWF (2012) section 3.6.2), plays an important role into achieving this good accuracy. Orography is subtracted from the advected mass field resulting in a much smoother field which can be accurately interpolated to the departure points.

Although total air mass conservation error in IFS is small, it turns to be much larger when individual tracers are considered. As NWP models become more complex and used as environmental prediction systems where large number of tracers are advected, the requirement for conservative schemes becomes more important. Furthermore, as the resolution increases towards cloud resolving scales, where accurate conservation of moisture at the local scale can be important for resolving buoyancy, it becomes increasingly desirable to have a mass conserving advection scheme.

Global mass conservation errors in tracer advection depend on the smoothness of the field, i.e. smoother fields such as ozone and specific humidity have much smaller conservation errors than fields with sharp features such as cloud fields. This is demonstrated in Fig. 7 where the global conservation error (as a percentage of the initial total mass of the advected tracer) is displayed for: ozone, specific humidity (Q), cloud liquid water content (CLWC), cloud ice water content (CIWC). A conservative scheme would have been represented in this plot by a line identical with the horizontal 0-axis; the closer to the horizontal axis a curve is the smaller the mass conservation error. In these experiments, parametrizations

have been switched off to isolate sources and sinks and allow testing the performance of the advection scheme in realistically complex terrain. The errors for the two cloud fields CLWC, CIWC have been assessed separately with the quasi-monotone, quasi-cubic ECMWF interpolation scheme and the linear interpolation scheme (indicated with LIN in plots). The former choice is used operationally in the model for Q and ozone and other aerosols while the later is used for the rougher cloud fields. The experiments are run at different horizontal and vertical resolutions: (i) T159 L60 i.e. T159 in the horizontal with 60 levels in the vertical (ii) T159 L91 (iii) T1279 L91 and (iv) T1279 L137. To allow direct comparisons of the per timestep mass conservation error, the four top forecasts in Fig. 7 have run for the same number of timesteps. At coarse horizontal resolution (T159) the timestep is 6 times longer (60 mins) than the corresponding timestep for high resolution (T1279).

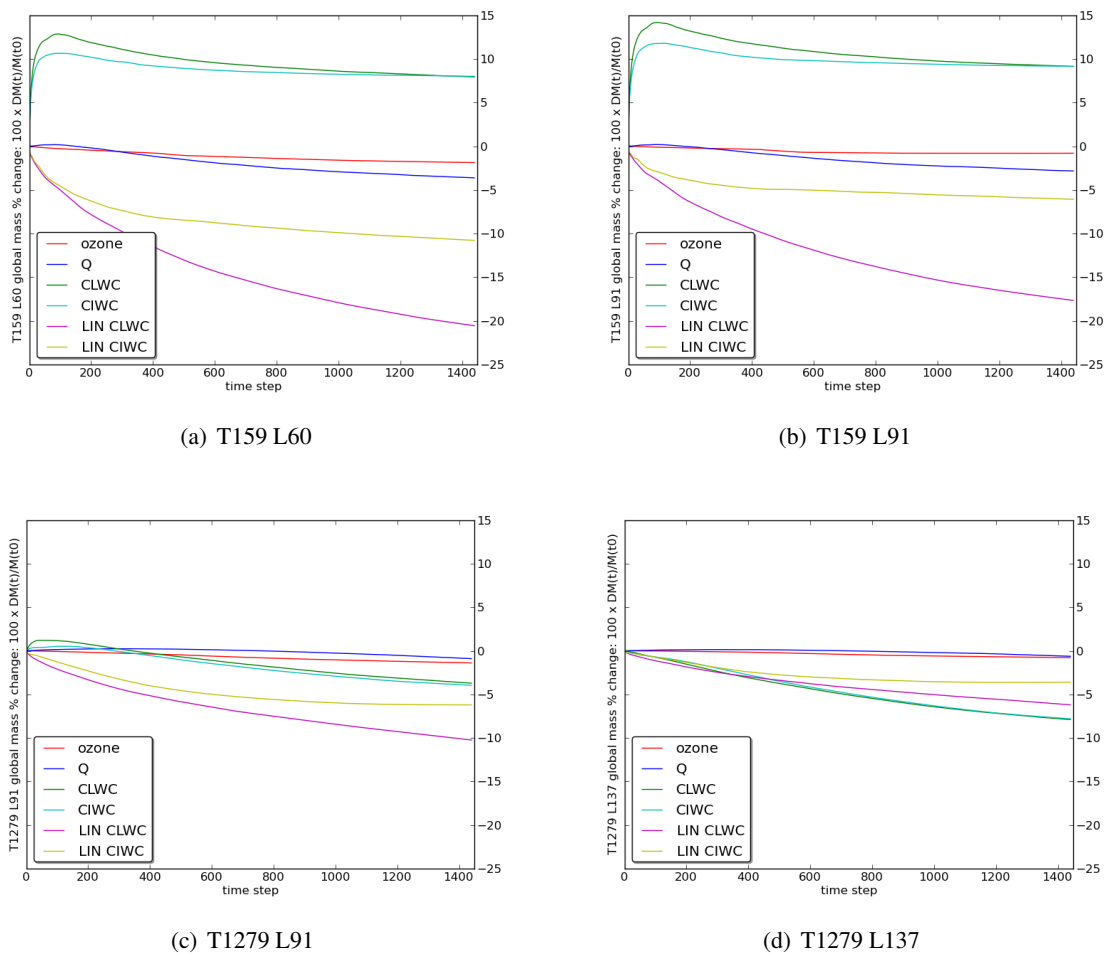


Figure 7: Global mass budgets for ozone, Q, CLWC, CIWC at different resolutions.

The overall impression from these results is that the global mass conservation error per timestep tends to decrease as the resolution increases. This may not be a precise statement for every tracer but gives a strong indication of a reduction of the error per timestep as resolution is refined especially when this error is large. So apart of the expected improvement in forecasting accuracy obtained with increased resolution an improvement in global mass conservation is achieved as well. For cubic interpolation, increase of horizontal resolution results to a noticeable reduction of the global tracer mass error, in particular for CLWC, CIWC. Increasing the vertical resolution seems to have a small positive impact for the smoother fields (Q, ozone). For the linearly interpolated fields, increasing vertical resolution, leads to a reduction of their global mass error. Increasing horizontal resolution improves 'LIN CLWC' but leaves relatively un-affected 'LIN CIWC' which is the most localised and least smooth.

5.1 The mass fixer approach

There is a class of semi-Lagrangian schemes, the so called inherently conserving schemes, which are able to achieve global, local and consistent mass conservation for all transported fields. Two typical examples are SLICE [Zerroukat and Allen \(2012\)](#) and CSLAM [Lauritzen et al. \(2010\)](#). Such schemes are essentially an application of a finite-volume type discretization approach on the semi-Lagrangian continuity equation. Despite having desirable theoretical properties these schemes are in general complex to implement for a three-dimensional set up which includes orography. Significant changes are required in the standard semi-Lagrangian formulation and the computational cost of these algorithms can easily double compared with traditional semi-Lagrangian schemes. However, this is an active area of research and although currently inherently conserving schemes are not used in forecasting operations, further improvements may enable their use in applications, especially when multiple tracers are transported. An example of a recent relevant development is given in the paper by [Sørensen et al. \(2013\)](#).

An alternative low computational cost approach which has been used for several years by semi-Lagrangian climate and atmospheric chemical transport models is the so called “mass fixer” algorithm. The practice is to perform first the standard semi-Lagrangian advection step, i.e. to find first the departure points, interpolate the advected field to them and finally to correct the solution in order to satisfy global mass conservation.

There is currently a range of mass fixer algorithms published in the literature. In general, any mass fixer will compute the global mass before and after the advection step (interpolation to the departure points) and calculate its difference which gives the global mass conservation error at this step. Once the mass conservation error has been computed, then a very small amount of mass is added or subtracted from each grid-point. The global sum of this correction is equal (having an opposite sign) to the global mass conservation error. A sensible strategy, used by several mass fixer algorithms, is to compute a correction which is proportional to the smoothness of the solution. A larger correction is computed in areas where the solution has large gradients and therefore the error is large and a very small correction where the solution is smooth and the error is small.

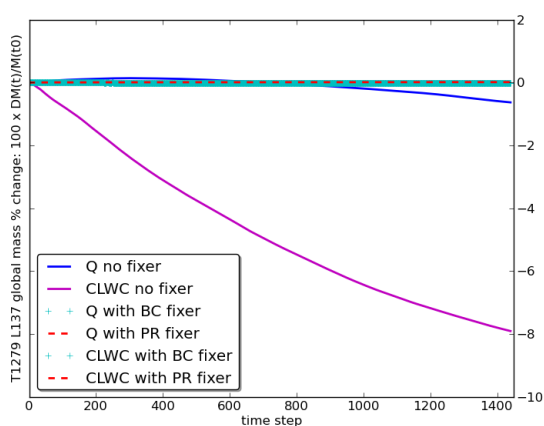


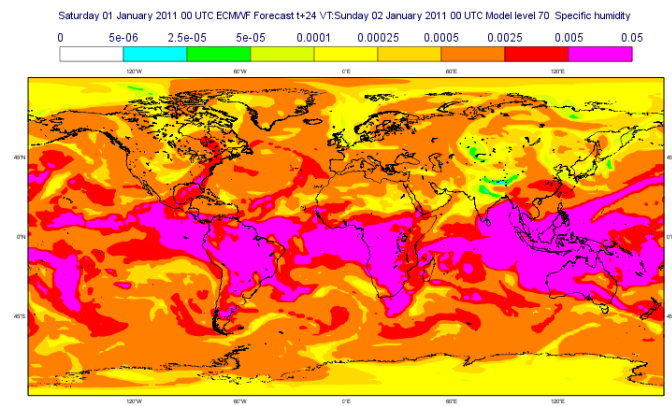
Figure 8: Global mass budgets for Q, CLWC at T1279 resolution forecast with/without mass fixers.

The following mass fixers have been recently implemented in IFS and are currently under evaluation:

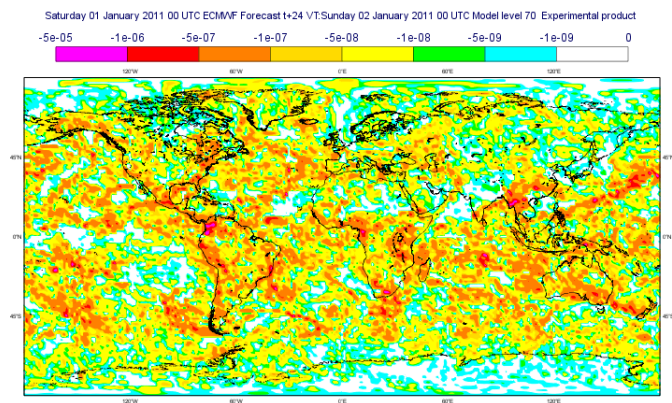
1. The quasi-monotone [Bermejo and Conde \(2002\)](#) algorithm.
2. The quasi-monotone [Priestley \(1993\)](#) algorithm.
3. [MacGregor \(2011\)](#) scheme originally developed for climate model C-CAM.

The first two of these fixers are using the mass correction strategy mentioned above while the third one is using a simpler lower cost strategy in which the correction is proportional to the advective increment and depends also on its sign. Details can be found in the respective references.

The impact of applying mass fixers on specific humidity (Q) and cloud liquid water content (CLWC) fields is demonstrated in Fig. 8. The global mass conservation error for the tracer drops to 0, i.e. the advection is now globally conserving. It is also interesting to see how the mass fixer acts locally. This can be seen in Fig. 9 where the correction field for Q at $t+24$ hrs forecast step, computed by the Bermejo & Conde fixer, is plotted. The fact that the increments are larger in areas of large gradients and very small where the field is smooth demonstrates that the local criterion used by the fixer achieves what is expected.



(a) Q field



(b) Fixer correction field

Figure 9: Mass fixer increment for the specific humidity field from Bermejo & Conde algorithm at step $t+24$ hrs and near 700 hPa height.

A natural area for applying mass fixers is applications where chemical species are transported. For such applications, it is additionally important to mass conservation that existing functional relationships in their concentration are maintained by the advection scheme (see [Lauritzen and Thuburn, 2012](#)). The

ability of IFS and the newly developed fixers to preserve such relationships has been tested using case 1.1 from DCMIP (Dynamical Core Model Intercomparison Project, see [Ulrich et al., 2012](#)). This is a three-dimensional passive advection deformational flow idealised test case in which four tracers are transported. The first two tracer fields q_1, q_2 are correlated by the non-linear relation:

$$q_2(\lambda, \theta, z) = 0.9 - 0.8q_1^2(\lambda, \theta, z)$$

where λ, θ, z is the longitude, latitude and height of a tracer. The first one is represented by two cosine bells placed at the same height and latitude but at different longitudes.

Results for this test case from IFS runs at T159 horizontal resolution and 137 levels in the vertical¹ are plotted in Fig. 10. These are correlation plots for the pair (q_1, q_2) at $t = 6$ days after the initial time (which is half the time required for the tracers to complete one full rotation around the earth). The initial concentration of these tracers is given by the parabolic part of the dash-dotted black curve. Pairs (q_1, q_2) , represented by red dots, falling outside the region indicated by the dashed-dotted convex envelope correspond to unphysical mixing ratios. Ideally, the red region should stay within the convex envelope and follow the curve closely, spreading evenly and thinly on it. Fig. 10 shows that semi-Lagrangian transport with linear interpolation is excessively diffusive but does not produce any unphysical mixing. The opposite is true when cubic Lagrange is used. Significant improvement can be noticed when the [Bermejo and Staniforth \(1992\)](#) quasi-monotone limiter is used. However, it does not eliminate completely the unphysical mixing. Using [Bermejo and Conde \(2002\)](#) or [Priestley \(1993\)](#) mass fixer algorithms improves further as it results in better preservation of the existing functional relationship. Mac Gregor's fixer did not show an improvement in this respect for this case.

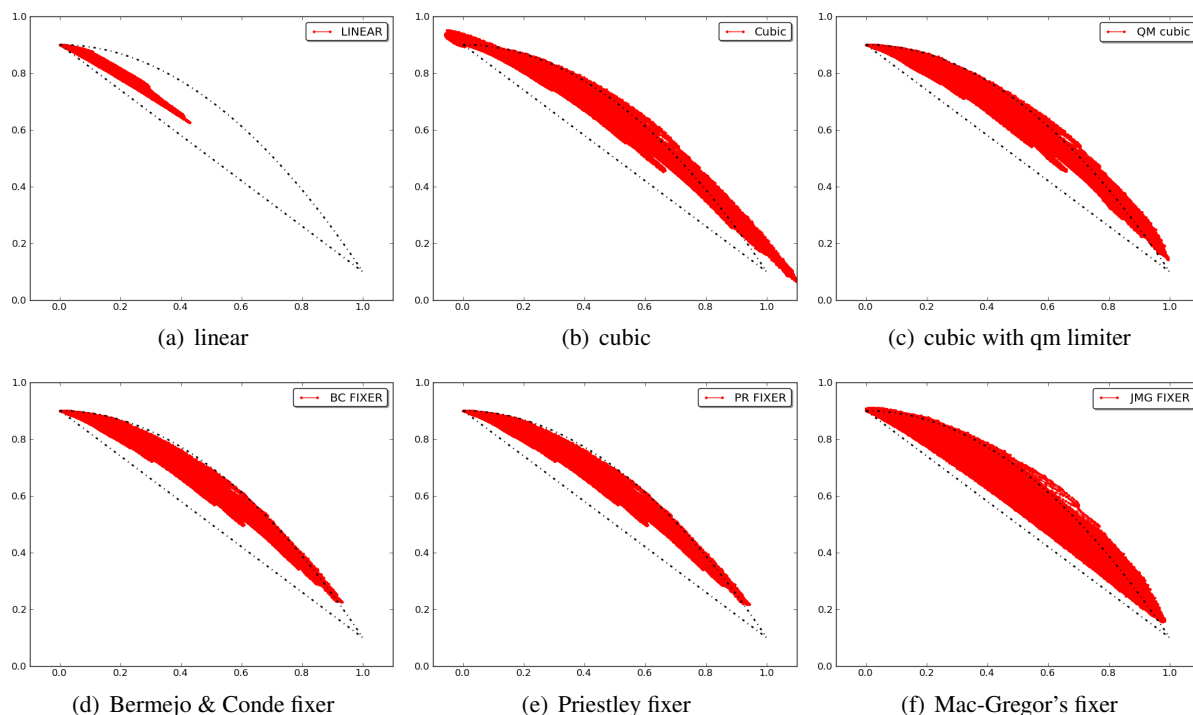


Figure 10: Scatter plots for tracers (q_1, q_2) at $t = 6$ days for an initial concentration which follows the upper black dashed-dotted curve.

Further testing of these algorithms has shown that for short and medium range NWP forecasts their impact in terms of skill scores is neutral while for long-range forecasts the impact on fields such as temperature is positive (reduced errors). These algorithms are currently tested to establish how they

¹This horizontal and vertical resolution is close to the recommended for this problem.

perform in environmental-chemical forecasts and to determine if a benefit can be found in high resolution non-hydrostatic scale forecasts.

6 Conclusions

The semi-Lagrangian, semi-implicit technique is an established numerical method in weather prediction and more generally in atmospheric modelling. Being a highly efficient technique it has enabled the implementation of robust high resolution NWP systems and has contributed in the improvement of weather forecasts.

As explained in this paper, apart of the great strengths of SLSI, there are some weak areas as well. Its theoretical unconditional stability is limited by time extrapolations used for computing the SL trajectories and for evaluating the non-linear right-hand side terms in the semi-implicit scheme. Systematic errors such as the extratropical tropopause cold temperature bias and lack of formal mass conservation are two other disadvantages. In ECMWF we are currently working on these long-standing issues aiming to improve accuracy and robustness of IFS at different resolutions and forecast timescales. Some relevant work has been summarized here showing potential for operational implementation. Research and development in this area continues and we hope to be able to implement further improvements in the near future.

Developments in atmospheric modelling follow developments in super-computing industry. As hardware manufacturers have stopped producing CPUs with faster clock speeds the only practical way to increase computing power and tackle larger size problems is through increased parallelism. In recent years there has been a gradual shift to massively parallel computing architectures and it is foreseen that exascale machines will be available for the meteorological community the next decade. The issue of scalability of numerical techniques currently used in atmospheric modelling is becoming a central one, especially as resolutions of global models are gradually shifting to scales not permitting the hydrostatic approximation. For such model resolutions and massively parallel architectures, latitude-longitude regular grids become highly anisotropic in physical space. For explicit Eulerian schemes this implies large restriction to the timestep which makes their use impractical. On the other hand, for semi-implicit schemes the main limiting factor is high cost of communication for implicit solvers and slow convergence rates.

For SLSI schemes on quasi-uniform grids, in particular for spectral transform methods on reduced Gaussian grids such as the IFS, the high cost of Legendre transforms is an important limiting factor. Recently [Wedi et al. \(2013\)](#) have shown how a significant reduction of this cost may be achieved. Despite these significant improvements, there are still outstanding issues. Two important ones are the high communication cost of global transpositions and the viability of the constant coefficient approach in the semi-implicit system. The latter offers the advantage of a very low computational cost Helmholtz solver but requires explicit handling of orographic forcing. Lack of formal conservation in traditional SL models, as opposed to Eulerian flux-form models, is a further drawback and currently an active research topic in the semi-Lagrangian community.

The question of how efficient the SL approach may be in future also depends on the type of forecast considered. For example for applications where many tracers are transported the semi-Lagrangian technique has an advantage as transport can be done very cheaply - there is no need to solve a prognostic equation for each tracer. All that is required is one interpolation per tracer to the departure points which are calculated only once per timestep.

The above discussion highlights that it is not easy to predict for how much longer the semi-Lagrangian approach will continue to be used in atmospheric modelling. However, on the basis of current knowledge, we can safely predict that the semi-Lagrangian IFS will be operating at least until the beginning

of next decade and will continue to deliver improved weather forecasts.

Acknowledgements

The author gratefully acknowledges the help of his colleagues in preparing this manuscript. Dr N. Borrmann for his assistance in evaluating the numerical scheme presented in section 3.3. Dr R. Forbes for discussions and help on evaluating IFS on the cold bias problem. Dr S. Malardel for providing her idealised code used for tests in section 5 as well as for useful comments on the manuscript. Dr A. Simmons for providing enlightening information and references regarding early stages of development of the semi-Lagrangian IFS.

References

- Bermejo, R. and J. Conde (2002). A conservative quasi-monotone semi-Lagrangian scheme. *Mon. Weather Rev.* 130, 423–430.
- Bermejo, R. and A. Staniforth (1992). The conversion of semi-Lagrangian advection schemes to quasi-monotone schemes. *Mon. Weather Rev.* 120, 2622–2631.
- ECMWF, R.-D. (2012). IFS documentation. <http://www.ecmwf.int/research/ifsdocs/>.
- Hortal, M. (2002). The development and testing of a new two-time-level semi-Lagrangian scheme (SETTLS) in the ECMWF forecast model. *Q.J.R. Meteorol. Soc.* 128, 1671–1687.
- Hortal, M. (2004, September). Overview of the numerics of the ECMWF atmospheric forecast model. In *Recent developments in numerical methods for atmospheric and ocean modelling*. ECMWF.
- Hyman, J. (1983). Accurate monotonicity preserving cubic interpolation. *SIAM J. Sci. and Stat. Comput.* 4, 645–654.
- Lauritzen, P., R. D. Nair, and P. A. Ullrich (2010). A conservative semi-Lagrangian multi tracer transport scheme (CSLAM) on the cubed-sphere grid. *J. Comput. Phys.* 229, 1401–1424.
- Lauritzen, P. and J. Thuburn (2012). Evaluating advection/transport schemes using interrelated tracers, scatter plots and numerical mixing diagnostics. *Q.J.R. Meteorol. Soc.* 138, 906–918.
- MacGregor, J. (2011). C-CAM geometric aspects and dynamical formulation. Technical Report 70, CSIRO Atmospheric Research, Aspendale, Vic.
- Priestley, A. (1993). A quasi-conservative version of the semi-Lagrangian advection scheme. *Mon. Weather Rev.* 121, 621–629.
- Pudikewicz, J., R. Benoit, and A. Staniforth (1985). Preliminary results from a partial Irtap model based on an existing forecast model. *Atmos. Ocean* 23, 267–303.
- Ritchie, H. and M. Tanguay (1996). A comparison of spatially averaged Eulerian and semi-Lagrangian treatment of mountains. *Mon. Weather Rev.* 124, 167–181.
- Ritchie, H., C. Temperton, A. Simmons, M. Hortal, T. Davies, D. Dent, and M. Hamrud (1995). Implementation of the semi-Lagrangian method in a high-resolution version of the ECMWF forecast model. *Mon. Weather Rev.* 121, 489–514.
- Simmons, A. (1991, September). Development of a high resolution, semi-Lagrangian version of the ecmwf forecast model. In *Seminar on Numerical Methods in Atmospheric Models*. ECMWF.

- Simmons, A. and D. Burridge (1981). An energy and angular momentum conserving vertical finite difference scheme and hybrid vertical coordinates. *Mon. Weather Rev.* 109, 758–766.
- Smolarkiewicz, P. and J. Pudykiewicz (1992). A class of semi-Lagrangian approximations for fluids. *J. Atmos. Sci.* 49, 2082–2096.
- Sørensen, B., E. Kaas, and U. Korsholm (2013). A comparison of spatially averaged Eulerian and semi-Lagrangian treatment of mountains. *Geosci. Model Dev.* 124, 1029–1042.
- Staniforth, A. and J. Côté (1991). Semi-Lagrangian integration schemes for atmospheric models - a review. *Mon. Weather Rev.* 119, 2206–2223.
- Stenke, A., V. Grewe, and M. Ponater (2008). Lagrangian transport of water vapor and cloud water in the ECHAM4 GCM and its impact on the cold bias. *Clim Dyn* 31, 491–506.
- Temperton, C., M. Hortal, and A. Simmons (2001). A two-time-level semi-Lagrangian global spectral model. *Q.J.R. Meteorol. Soc.* 127, 111–127.
- Ulrich, P., C. Jablonowski, J. Kent, P. Lauritzen, R. Nair, and M. Taylor (2012). Dynamical Core Model Intercomparison Project (DCMIP) test case document. Technical report, NCAR.
- Wedi, N., M. Hamrud, and G. Mozdzynski (2013). A fast spherical harmonics transform for global NWP and climate models. *Mon. Weather Rev.* 141, 3450–3461.
- Zerroukat, M. and T. Allen (2012). A three-dimensional monotone and conservative semi-Lagrangian scheme (SLICE-3D) for transport problems. *Q.J.R. Meteorol. Soc.* 138, 1640–1651.